



Mesophase pitch production aided by the thermal decomposition of polyvinylidene fluoride

Chaehun Lim¹ · Yoonyoung Ko² · Cheol Hwan Kwak² · Seokjin Kim¹ · Young-Seak Lee^{1,2}

Received: 31 May 2022 / Revised: 19 June 2022 / Accepted: 21 June 2022 / Published online: 7 July 2022
© The Author(s), under exclusive licence to Korean Carbon Society 2022

Abstract

The facile production of high-purity mesophase pitch has been a long-standing desire in various carbon industries. Recently, polymer additives for mesophase production have attracted much attention because of their convenience and efficiency. We propose polyvinylidene fluoride (PVDF) as a strong candidate as an effective additive for mesophase production. The mesophase content and structural, chemical, and thermal properties of pitches obtained with different amounts of added PVDF are discussed. The influence of PVDF decomposition on mesophase formation is also discussed. We believe that this work provides an effective option for mesophase pitch production.

Keywords Mesophase pitch · Fluorination · Anisotropic carbon · Polymer additive

1 Introduction

Since mesophase pitch was identified by Brooks and Taylor, it has attracted considerable attention as the precursor of conductive carbon materials such as carbon fiber, artificial graphite, and anode materials used in lithium-ion batteries due to its anisotropy and graphitizable nature [1–4]. Mesophase pitch is prepared from polyaromatic hydrocarbon sources such as petroleum residue, coal tar, and single-component aromatic compounds [2, 5, 6]. Petroleum residue-based mesophase pitch has been studied intensively because of its abundance and affordable price. However, high-purity mesophase pitch is difficult to obtain by the simple pyrolysis of petroleum residue sources. Researchers worldwide have paid attention to additive-assisted reactions for the production of highly anisotropic petroleum-based mesophase pitch. There are many additives that can effectively produce mesophase pitch, such as inorganic additives, polymeric additives, and hydrocarbon fractions [7–13]. Halogen-based additives have shown remarkable performance by providing active

ions for dehydrogenation [10–12]. However, in many cases, they require tedious purification steps. Polymer-based additives have advantages in terms of convenience because they basically decompose and gasify at mesophase-producing temperatures [7–9]. In other words, polymeric additives do not need any impurity removal steps. Many researchers and members of the carbon industry are eager to find highly effective and highly convenient additives for mesophase pitch production.

In this work, we suggest PVDF as an effective and expedient additive for mesophase production. The structural, chemical, and thermal differences of pristine pitch and PVDF-aided pitch were comprehensively discussed. The effect of PVDF on mesophase formation and its mechanism were suggested. We hope this research will inspire new techniques for mesophase pitch production.

2 Experimental

2.1 Materials used

Fluid catalytic decant oil (FCC-DO) was provided by the Hyundai Oilbank (South Korea). PVDF (average molecular weight of 530,000 g/mol) was purchased from Sigma-Aldrich (USA).

✉ Young-Seak Lee
youngslee@cnu.ac.kr

¹ Department of Chemical Engineering and Applied Chemistry, Chungnam National University, Daejeon 34134, Republic of Korea

² Institute of Carbon Fusion Technology (InCFT), Chungnam National University, Daejeon 34134, Republic of Korea

2.2 Preparation of pitch

The pitches were produced under the following pyrolysis conditions. FCC-DO was pyrolyzed at 430 °C for 8 h in a N₂ atmosphere. The heating rate was 2 °C/min, and the nitrogen flow rate was 100 cc/min. The as-prepared pitch was named 430-8. The PVDF-aided pitches were prepared from a mixture of FCC-DO and PVDF. The PVDF mixtures were pyrolyzed under the same conditions mentioned above. The PVDF-assisted pitches were named 430-8-FPX, where X is the weight percentage of PVDF in the mixture of PVDF and FCC-DO.

2.3 Material characterization

The structural analysis of the prepared pitches was conducted with X-ray diffraction (XRD) and Raman spectroscopy. XRD was conducted with a D8 Advance spectrometer (Bruker, USA) with Cu K α radiation. Raman spectroscopy was performed with a LabRAM HR-800 (Horiba, Japan) with a 514 nm excitation laser. The chemical composition of the pitches was examined with X-ray photoelectron spectroscopy (XPS, K-alpha+, Thermo Fisher Scientific, USA) and elemental analysis (EA, Flash2000 and EA1112, Thermo Fisher Scientific, USA). The thermal properties of the pitches were analyzed with a TGA/DSC1 instrument (Metler Toledo, USA). The heating range was 30–1000 °C under a nitrogen atmosphere, and the heating rate was 5 °C/min. The softening point of the pitches was estimated with a DP90 (Metler Toledo, USA) according to the procedures of ASTM3461. The content of toluene insoluble (TI) and quinoline insoluble (QI) is evaluated according to ASTM D4312-95 and ASTM D4746-14, respectively. The *d*-spacing (*d*₀₀₂) and vertical stacking height of the carbon layer (*L*_C) were calculated with XRD data using Bragg's equation and Scherrer–Warren's equation below.

$$n\lambda = 2d \sin \theta, \quad (1)$$

$$L_c = \frac{0.89\lambda}{\beta \cos \theta}, \quad (2)$$

where θ is the peak position of the (002) peak, λ is the wavelength of the incident beam, and β is the full width at half maximum of the (002) peak.

3 Results and discussion

Structural analysis was conducted with XRD and Raman spectroscopy, as shown in Fig. 1a, b. The structural parameters, such as the *d*₀₀₂, *L*_C, and *I*_D/*I*_G values, were calculated and are presented in Table 1. Figure 1a and Table 1 show that the interlayer spacing *d*₀₀₂ slightly decreases with the proportion of PVDF in the raw material. The lateral crystal sizes of the pitches, *L*_C, were significantly increased upon addition of PVDF. The *L*_C value of the 430-8-FP2.1 sample was approximately 2.6 times larger than that of the pristine 430-8 sample. The PVDF-assisted reaction seems more helpful for constructing larger crystallites than for narrowing the interlayer space. Moreover, the *I*_D/*I*_G values of the as-prepared pitches decreased as PVDF was added. This means that the addition of PVDF promotes the formation of carbon planes with fewer defects [14, 15]. From the structural data obtained from XRD analysis and Raman spectra, it is clear that the addition of PVDF in the pitch synthetic reaction can help form larger and more ordered carbon structures than the pristine pitch producing method. In detail, the PVDF decomposition reaction results in large and well-ordered crystalline pitch.

The chemical and thermal properties of the pitches are presented in Fig. 2. The corresponding analysis values are arranged in Table 2. From the EA data in Fig. 2a and Table 2, the carbon content increased with the amount of added PVDF, while the amount of hydrogen decreased. Accordingly, the molecular ratio *C*/*H* increased as more PVDF was added, as shown in Fig. 2a. This seems to be because PVDF assisted in forming a carbon structure by promoting the dehydrogenation reaction. These results support the structural improvement by the PVDF-assisted reaction confirmed by XRD and Raman spectra.

The TGA curves of the pitches used in this study are shown in Fig. 2b. The weight losses at temperatures of approximately 200–300 °C are defined as the vaporization of volatile compounds in the pitches, and the weight loss at 400–600 °C is often considered as dehydrogenation and dealkylation in the coking reaction [16]. The resulting carbonization yields of pitches in Table 2 imply that PVDF addition can improve the thermal stability of the resulting pitches. In addition, the softening point of the pitches significantly increased with the addition of PVDF; the 430-8-FP0.7 sample had a 117.1 °C higher softening point than that of

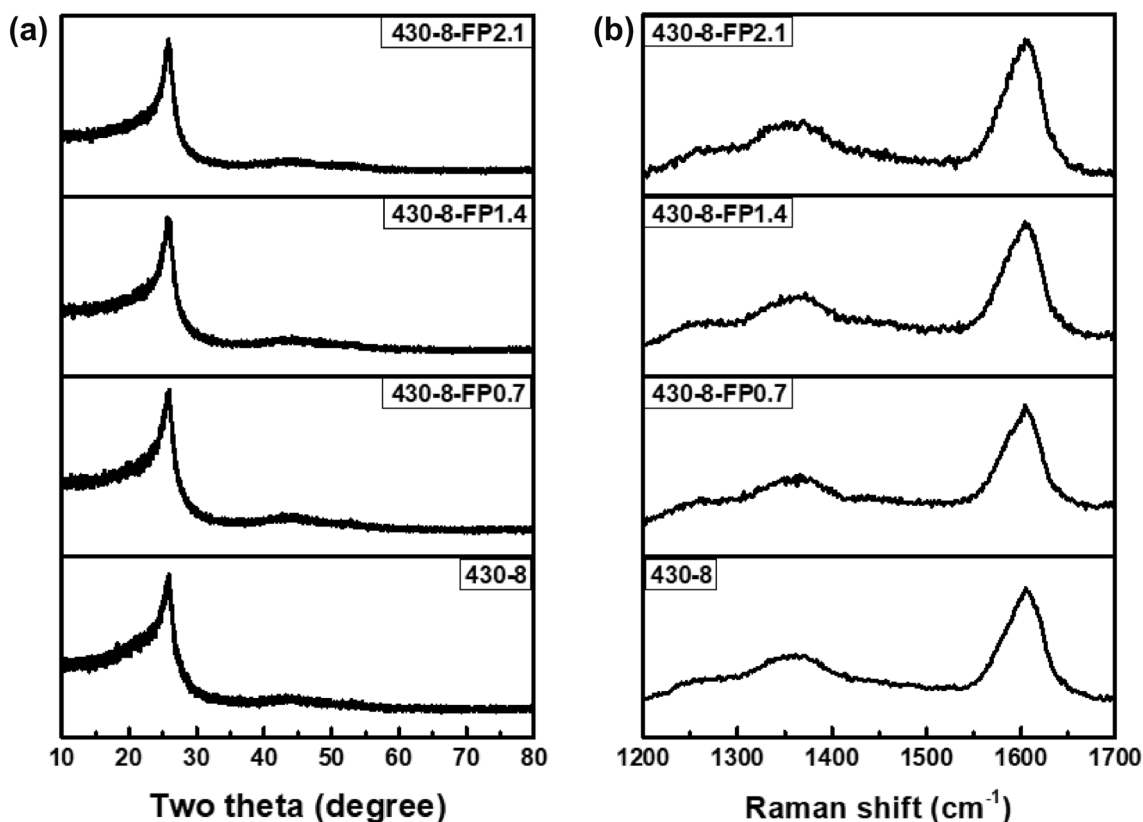


Fig. 1 XRD data (a) and Raman spectra (b) of the prepared pitches

Table 1 Structural parameters of the prepared pitches

| Sample | d_{002} (nm) | L_c (nm) | I_D/I_G |
|-------------|----------------|------------|-----------|
| 430-8 | 3.459 | 9.09 | 0.67 |
| 430-8-FP0.7 | 3.458 | 22.45 | 0.65 |
| 430-8-FP1.4 | 3.454 | 22.63 | 0.64 |
| 430-8-FP2.1 | 3.452 | 24.00 | 0.61 |

the pristine pitch. The softening points of the 430-8-FP1.4 and 430-8-FP2.1 samples were not detected, so considering the TGA results, those samples were considered to be the intermediate of mesophase pitch and cokes. Considering the structural analysis, the large and well-ordered structure achieved by the PVDF-assisted reaction affected the thermal stability and softening behavior with the large molecular size and stronger bonding.

The XPS survey spectra of the as-prepared pitches are presented in Fig. 2c to evaluate the presence of remaining PVDF and fluorine functional groups. In the XPS spectra,

no fluorine peaks were observed even for the 430-8-FP2.1 sample. According to prior research, PVDF with a similar molecular weight used in this study starts to decompose at approximately 410 °C under inert conditions, and heat treatment at 430 °C for 8 h seems sufficient to degrade all of the added PVDF [17, 18]. This is an advantageous result because PVDF-aided pitches do not need any purification steps. The chemical and thermal analyses from EA and TGA agreed with the structural analysis, and the XPS spectra demonstrated an additional advantage of the PVDF-assisted reaction.

The polarized images of the as-prepared pitches are shown in Fig. 3. As seen by comparing the pristine pitch with the PVDF-assisted pitches, the PVDF-assisted pitches contained overwhelmingly large mesophase domains. This mesophase domain is comparable to those obtained via halogenating catalyst-assisted reactions involving FeCl_3 , AlCl_3 , and HF/BF_3 [10–12]. The 430-8 sample had a large proportion of isotropic regions, and only 0.7 weight percent PVDF resulted in nearly fully grown mesophase domains.

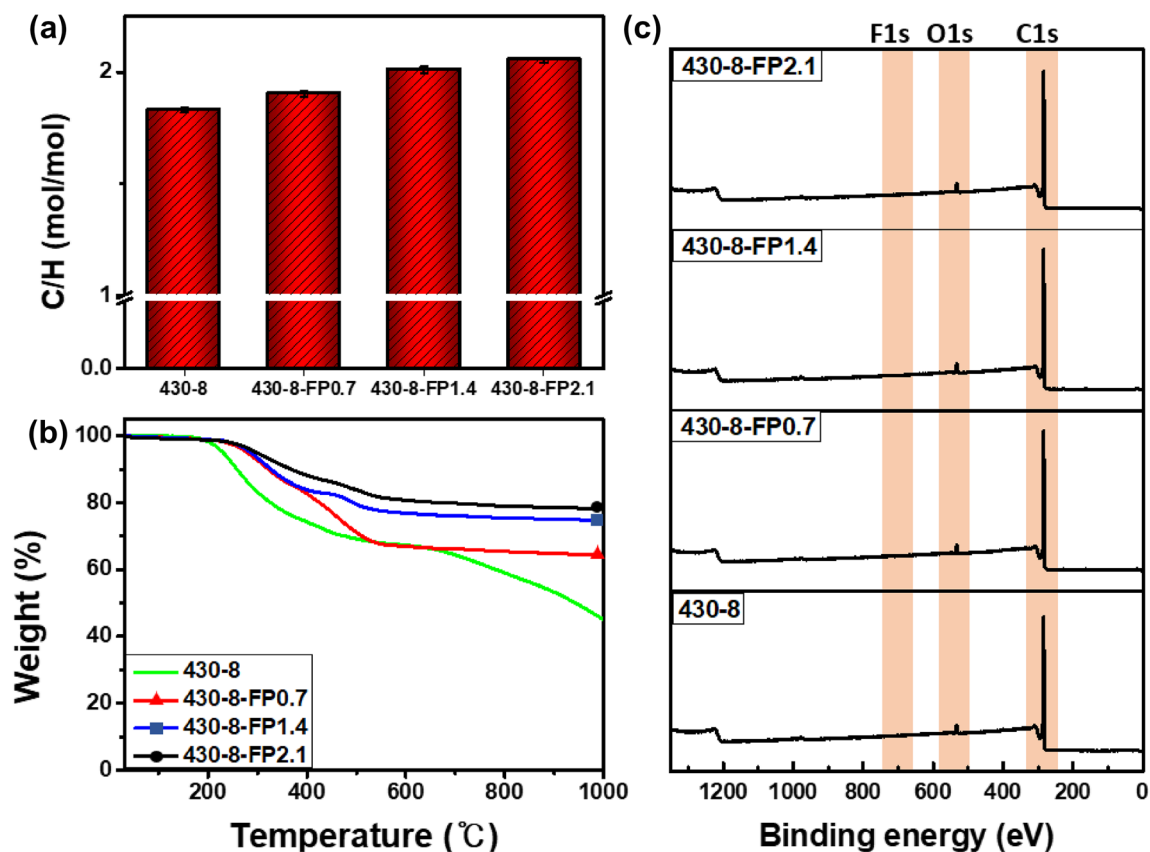


Fig. 2 C/H ratio (a), TGA curves (b), and XPS survey spectra (c) of the prepared pitches

The 430-8-FP2.1 sample exhibited a full anisotropic texture, which can be found in needle cokes. The 430-8-FP0.7 sample with a softening point of 313 °C could be applied to conductive mesophase pitch-based carbon fibers. Furthermore, the 430-8-FP1.4 and 430-8-FP2.1 samples could be used as filler materials for high-quality graphite materials. We expect that the anisotropic texture and structural and thermal properties can be controlled by modifying variables such as the reaction temperature, reaction time, amounts of additives, and types of additives similar to PVDF to comply with the specifications for their applications. The advantage of this result is that the PVDF-assisted reaction produces large domain mesophase pitch and needle cokes with the addition of a small amount of PVDF and no need for any post-treatments.

The manufacturing yield and solvent solubilities of pitches in Table 2 support the thermal stabilities and mesophase contents. As the amount of added PVDF increases, the QI components increased. This is because of the increase of large molecular mesophase content. And the increase of thermally stable QI components can be directly connected to increase in carbonization yield. While mesophase content and carbonization yield were drastically increased by addition of 0.7% of PVDF, the manufacturing yield decreased only 3.7%. From this result, we expect that the effect of decomposed PVDF is the acceleration of polymerization rather than the volatilization of the light components. And from the polymerizing effect, contents of the heavy fraction referred as QI drastically increased along the added amount of PVDF.

Table 2 Chemical compositions, carbonization yields, and softening points of the prepared pitches

| Sample | Yield (%) | SP (°C) | CY ^a (wt%) | C (wt%) | H (wt%) | O (wt%) | N (wt%) | S (wt%) | C/H (mol/mol) | TS (wt%) | TI-QS (wt%) | QI (wt%) |
|-------------|-----------|-------------------|-----------------------|---------|---------|---------|---------|---------|---------------|----------|-------------|----------|
| 430-8 | 57.4 | 196.4 | 45.1 | 92.85 | 4.23 | 0.47 | 0.60 | 0.50 | 1.83 | 21 | 44.2 | 34.8 |
| 430-8-FP0.7 | 53.7 | 313.5 | 64.5 | 92.93 | 4.07 | 0.38 | 0.60 | 0.50 | 1.90 | 9.4 | 27.4 | 63.2 |
| 430-8-FP1.4 | 52.5 | N.D. ^b | 74.8 | 92.95 | 3.98 | 0.40 | 0.57 | 0.47 | 2.01 | 3.7 | 17.8 | 78.5 |
| 430-8-FP2.1 | 48.6 | N.D. | 78.4 | 92.98 | 3.77 | 0.42 | 0.55 | 0.45 | 2.06 | 2.3 | 11 | 86.7 |

^aCarbonization yield^bNot detected

The schemes for the overall process for the PVDF-assisted production of mesophase pitch are demonstrated in Fig. 4a. We suggest that fluorine radicals decomposed from the heat treatment of PVDF-assisted polymerization of FCC-DO to create mesogens, and then, these mesogens acted as mesophase seeds to produce a large domain mesophase pitch. The specific reaction pathways are suggested, as demonstrated in Fig. 4b. The reaction mechanisms were referenced from the dehydrogenation reaction by halogenation using chlorine- and boron-based catalysts [19, 20]. First, PVDF decomposes upon heat treatment, and fluorine radicals are generated. Then, the fluorine radicals dehydrogenate polyaromatic hydrocarbons in FCC-DO. The dehydrogenated sites of polyaromatic hydrocarbons act as radical active sites. Polyaromatic hydrocarbons with more radical active sites easily react with each other by radical termination reactions. Through this radical polymerization, polymerized large molecular polyaromatic hydrocarbons can serve as mesophase seeds, and these mesophase seeds promote spherical mesophase formation. This spherical mesophase, called mesogen, grows as pyrolysis progresses. Then, the as-grown mesogens coalesce with each other to form bulky mesophase junk. The fully grown mesophase gradually develops a flow domain texture [21–24]. The HF synthesized from dehydrogenation may vaporize and degas because it has a low boiling point of 19.5 °C, and/or it may decompose and react to generate H₂ and F₂ gas. Then, H₂ is degassed, and F₂ undergoes an additional radical chain reaction because F₂ forms radicals even at room temperature [25–29]. It is considered that the byproducts from this reaction are all in the gas phase at the reaction temperature, so the resulting pitches do not have impurities.

4 Conclusion

We proposed PVDF-assisted production of mesophase pitch and its reaction mechanism based on dehydrogenation by radical chain reaction. The resulting PVDF-aided samples had larger and more ordered structures than the pristine pitch. Accordingly, the PVDF-assisted samples presented higher thermal stabilities than the pristine pitch. Consistent with the structural and thermal properties, the PVDF-added samples exhibited a much larger mesophase domain than the pristine samples. Moreover, the PVDF-assisted reaction did not produce impurities, so additional purification could be avoided. With these results, we strongly recommend PVDF as an additive for mesophase production because it is as effective as halogen-based catalysts and does not leave any traces as other polymer additives.

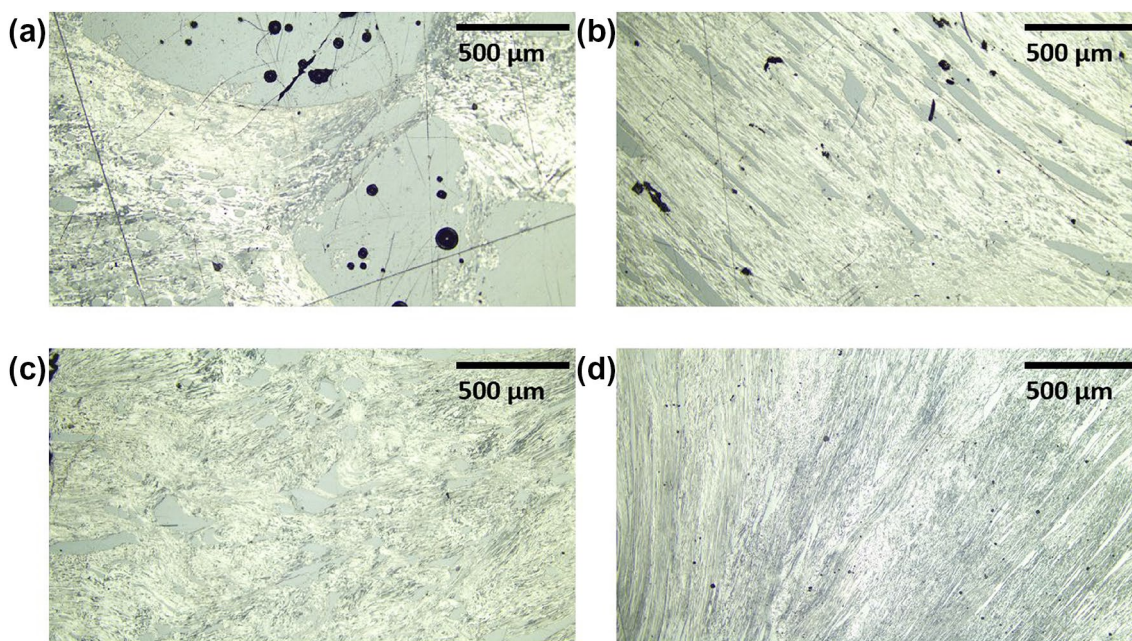


Fig. 3 Polarized images of the 430-8 (a), 430-8-FP0.7 (b), 430-8-FP1.4 (c), and 430-8-FP2.1 (d) samples

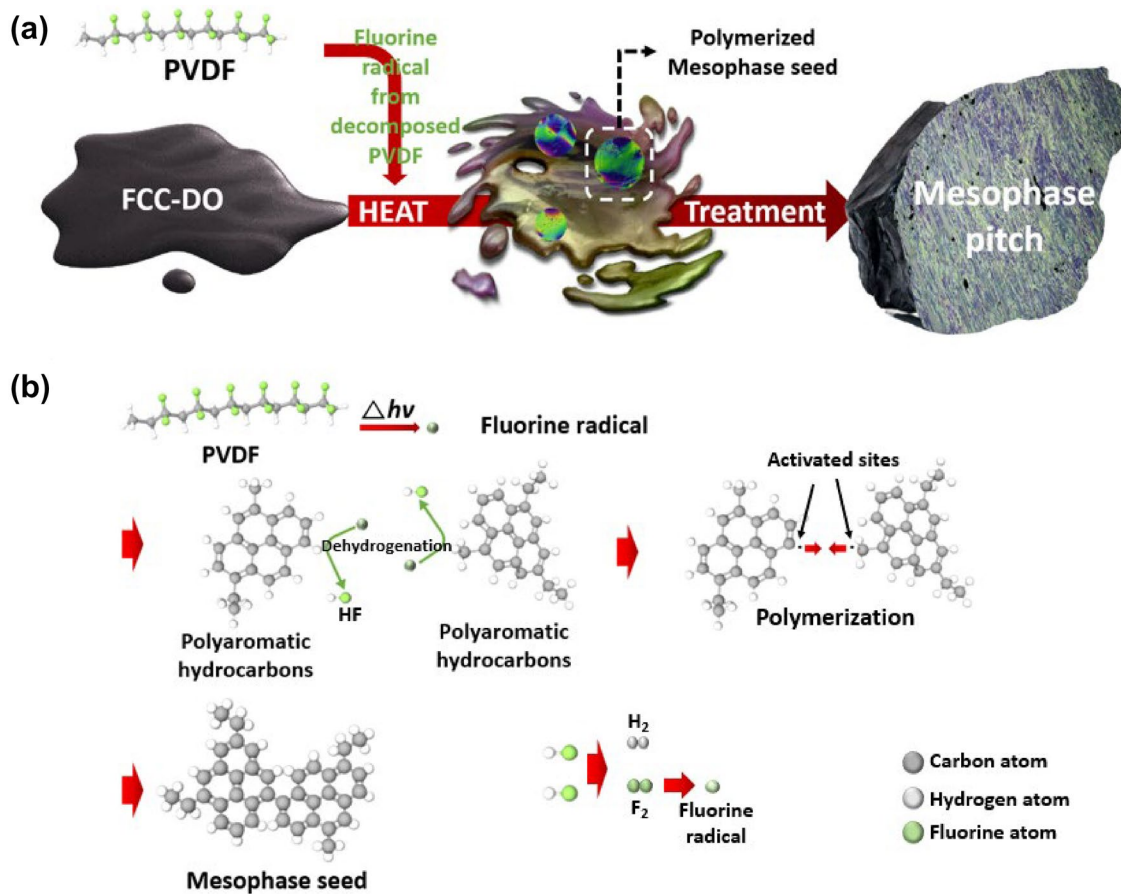


Fig. 4 Schematic of the overall reaction (a) and the reaction mechanism (b) of the PVDF-assisted mesophase formation reaction

Acknowledgements This work was supported by the Carbon Cluster Construction Program (10083586, Development of petroleum based graphite fibers with ultrahigh thermal conductivity) funded by the Ministry of Trade, Industry & Energy (MOTIE, Korea)

Declarations

Conflict of interest No potential conflict of interest relevant to this article was reported.

References

- Brooks JD, Taylor GH (1965) The formation of graphitizing carbons from the liquid phase. *Carbon* 3:187–193
- Ko S, Choi JE, Lee CW, Jeon YP (2019) Preparation of petroleum-based mesophase pitch toward cost-competitive high-performance carbon fibers. *Carbon Lett* 30:35–44
- Lee SE, Kim JH, Lee YS, Bai BC, Im JS (2020) Effect of crystallinity and particle size on coke-based anode for lithium ion batteries. *Carbon Lett* 31:911–920
- Lee SM, Kang DS, Roh JS (2015) Bulk graphite: materials and manufacturing process. *Carbon Lett* 16:135–146
- Banerjee C, Chandaliya VK, Dash PS (2021) Recent advancement in coal tar pitch-based carbon fiber precursor development and fiber manufacturing process. *J Anal Appl Pyrolysis* 158:105272
- Jiao S, Guo A, Wang F, Chen K, Liu H, Ibrahim UK, Wang Z, Sun L (2020) Effects of olefins on mesophase pitch prepared from fluidized catalytic cracking decant oil. *Fuel* 262:116671
- Kim JH, Choi YJ, Lee SE, Im JS, Lee KB, Bai BC (2021) Acceleration of petroleum based mesophase pitch formation by PET (polyethylene terephthalate) additive. *J Ind Eng Chem* 93:476–481
- Machnikowski J, Machnikowska H, Brzozowska T, Zieliński J (2002) Mesophase development in coal-tar pitch modified with various polymers. *J Anal Appl Pyrolysis* 65:147–160
- Cheng X, Zha Q, Li X, Yang X (2008) Modified characteristics of mesophase pitch prepared from coal tar pitch by adding waste polystyrene. *Fuel Process Technol* 89:1436–1441
- Mochida I, Shimizu K, Korai Y, Otsuka H, Sakai Y, Fujiyama S (1990) Preparation of mesophase pitch from aromatic hydrocarbons by the aid of HFBF_3 . *Carbon* 28:311–319
- Mochida I, Sone Y, Korai Y (1985) Preparation and properties of carbonaceous mesophase-II highly soluble mesophase from ethylene tar modified using aluminum chloride as a catalyst. *Carbon* 23:175–178
- Alain E, Begin D, Furdin G, Mareche JF (1996) Effect of graphite or FeCl_3 -graphite intercalation compounds on the mesophase development in coal tar pitch. *Carbon* 34:931–938
- Kim JH, Kim JG, Lee KB, Im JS (2019) Effects of pressure-controlled reaction and blending of PFO and FCC-DO for mesophase pitch. *Carbon Lett* 29:203–212
- Chadha N, Sharma R, Saini P (2021) A new insight into the structural modulation of graphene oxide upon chemical reduction probed by Raman spectroscopy and X-ray diffraction. *Carbon Lett* 31:1125–1131
- Schuepfer DB, Badaczewski F, Guerra-Castro JM, Hofmann DM, Heiliger C, Smarsly B, Klar PJ (2020) Assessing the structural properties of graphitic and non-graphitic carbons by Raman spectroscopy. *Carbon* 161:359–372
- Pérez M, Granda M, Garcia R, Santamaria R, Romero E, Menéndez R (2002) Pyrolysis behaviour of petroleum pitches prepared at different conditions. *J Anal Appl Pyrolysis* 63:223–239
- Gopika MS, Bindhu B, Sandhya KY, Reena VL (2019) Impact of surface-modified molybdenum disulphide on crystallization, thermal and mechanical properties of polyvinylidene fluoride. *Polym Bull* 77:757–773
- Orooji Y, Jaleh B, Homayouni F, Fakhri P, Kashfi M, Torkamany MJ, Yousefi AA (2020) Laser ablation-assisted synthesis of poly(vinylidene fluoride)/Au nanocomposites: crystalline phase and micromechanical finite element analysis. *Polymers* 12:2630
- Gabdulkhakov RR, Rudko VA, Pyagay IN (2022) Methods for modifying needle coke raw materials by introducing additives of various origin (review). *Fuel* 310:122265
- Dong Y, Xing G, Jin L, Li P, Cao Q (2019) Co-carbonization of brominated petroleum pitch, coal tar pitch and benzoyl chloride to prepare cokes. *New Carbon Mater* 34:258–266
- Halim HP, Im JS, Lee CW (2013) Preparation of needle coke from petroleum by-products. *Carbon Lett* 14:152–161
- Greinke RA, Singer LS (1988) Constitution of coexisting phases in mesophase pitch during heat treatment: mechanism of mesophase formation. *Carbon* 26:665–670
- Subhash K, Manoj S (2015) Mesophase formation behavior in petroleum residues. *Carbon Lett* 16:171–182
- Mochida I, Korai Y, Ku CH, Watanabe F, Sakai Y (2000) Chemistry of synthesis, structure, preparation and application of aromatic-derived mesophase pitch. *Carbon* 38:305–328
- Kim KH, Cho JH, Hwang JU, Im JS, Lee YS (2021) A key strategy to form a LiF-based SEI layer for a lithium-ion battery anode with enhanced cycling stability by introducing a semi-ionic C-F bond. *J Ind Eng Chem* 99:48–54
- Ha S, Lim C, Lee YS (2022) Fluorination methods and the properties of fluorinated carbon materials for use as lithium primary battery cathode materials. *J Ind Eng Chem*. <https://doi.org/10.1016/j.jiec.2022.03.044>
- Lee MH, Kim HY, Kim J, Han JT, Lee YS, Woo JS (2019) Influence of oxyfluorinated graphite on fluorinated ethylene-propylene composites as bipolar plates. *Carbon Lett* 30:345–352
- Padamata SK, Yasinskiy A, Stopic S, Friedrich B (2022) Fluorination of two-dimensional graphene: a review. *J Fluor Chem* 255–256:109964
- Apopian JC, Téraube O, Charlet K, Dubois M (2021) A review about the fluorination and oxyfluorination of carbon fibres. *J Fluor Chem* 251:109887

Publisher's Note Springer Nature remains neutral with regard to jurisdictional claims in published maps and institutional affiliations.